

Supporting Information for

NMR Spin-Lock Induced Crossing (SLIC) Dispersion and Long-Lived Spin States of Gaseous Propane at Low Magnetic Field (0.05 T)

Danila A. Barskiy^{*,a,b}, Oleg G. Salnikov^{c,d}, Alexey S. Romanov^{c,d}, Matthew A. Feldman^{a,b}, Aaron M. Coffey^{a,b}, Kirill V. Kovtunov^{c,d}, Igor V. Koptyug^{c,d}, Eduard Y. Chekmenev^{*,a,b,e,f,g}

^aInstitute of Imaging Sciences, Vanderbilt University, Nashville, TN 37232, USA

^bDepartment of Radiology, Vanderbilt University, Nashville, TN 37232, USA

^cInternational Tomography Center, 3A Institutskaya st., Novosibirsk, Russia

^dNovosibirsk State University, 2 Pirogova st., Novosibirsk, Russia

^eDepartment of Biomedical Engineering, Vanderbilt University, Nashville, TN 37232, USA

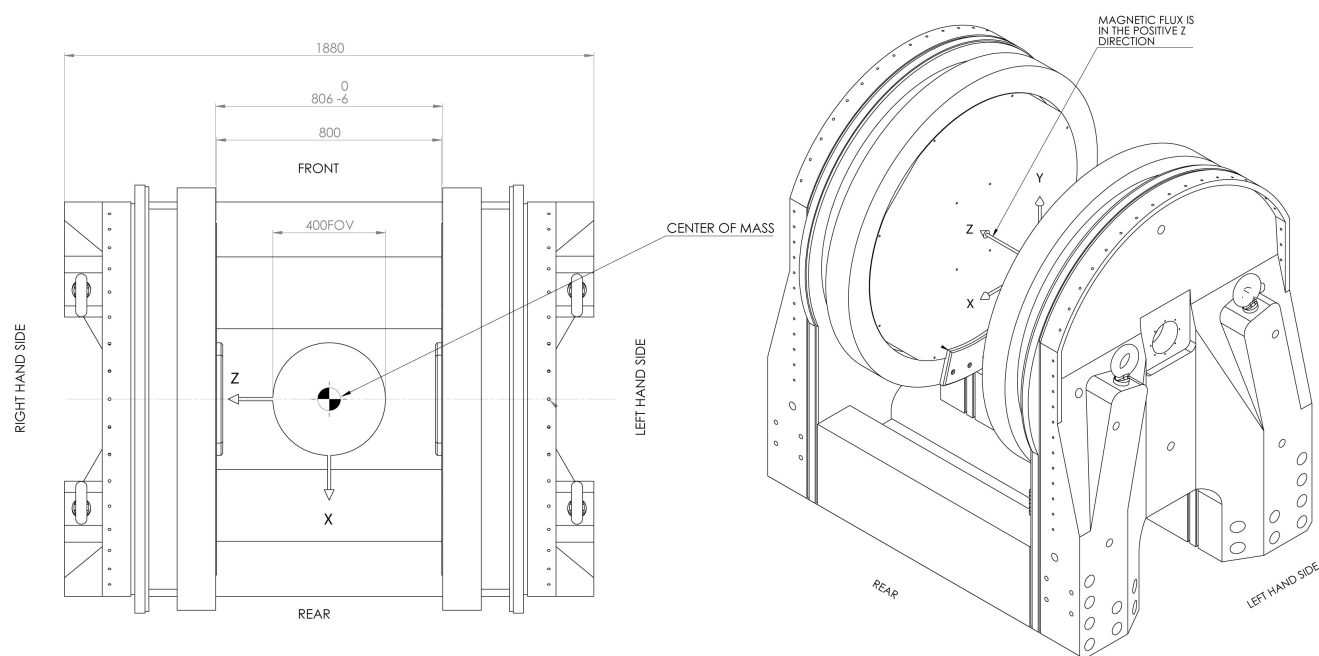
^fVanderbilt Ingram Cancer Center, Vanderbilt University, Nashville, TN 37232, USA

^gRussian Academy of Sciences, Moscow, Russia

Table of Contents

1. Additional information about the permanent magnet and the RF coil design.....	S-2
2. Spin dynamics calculations for the action of SLIC on propane.....	S-4
3. Analytical analysis of the ¹ H NMR signal vs. SLIC duration at 0.05 T.....	S-7
4. Values for T_1 and T_S and reaction conversion at different pressures.....	S-8
5. MatLab code used for the spin dynamics calculations.....	S-9
6. References Used in Supporting Information	S-11

1. Additional information about the permanent magnet and the RF coil design



Scheme S1. Configuration of the permanent magnet (~ 0.05 T) with 400 mm homogeneous field of view (FOV). Key dimensions are provided in millimeters.

Our experimental low field NMR apparatus is comprised of approximately 0.05 T (2.07 MHz actual ^1H frequency) permanent magnet and a dual-channel $^1\text{H}/^1\text{H}$ RF probe. The magnet has an 80 cm gap between the magnet plates (Scheme S1), and it has a homogeneity of <20 ppm across a 40 cm diameter of spherical volume (DSV) (Scheme S1). The magnet homogeneity was achieved using neodymium shim magnets in five sizes. The homogeneity can be further improved by driving a DC offset current through three orthogonal magnetic field gradient coils. The console used to perform NMR experiments was a dual-channel Kea2 (Magritek, Wellington, New Zealand) in low frequency configuration/mode.

A dual-channel NMR probe has two separate RF inductors with two independent tuning and matching circuits sharing the same ground (Figure S1a). It was built to measure samples placed in standard 5 mm outside diameter NMR tubes with the possibility to transmit and detect on different channels. The RF circuit tuning and matching networks were constructed from Johansen trimmer capacitors (1-30 pF, #5602) to tune the center frequency and the power match the coil. The circuit design for both coils was a parallel LC resonator with a series capacitive matching element (Figure S1a). The internal solenoid (Rx) was decoupled from the outer saddle-shaped coil (Tx) by orienting them orthogonally to achieve mutual orthogonality of B_1 fields of each RF coil to the main B_0 field (Figure S1b). Using the outer saddle coil, RF pulses can be transmitted to excite the spin system and the inner solenoid coil can be used to receive the signal by the spectrometer's receiving network. To increase the SNR, the inner solenoid coil matched the dimensions of the NMR sample (8 mm O. D., 193 mm length) thereby improving the filling factor of the inductor. The solenoid had ~ 800 windings, and it was constructed using 0.22 mm diameter

magnet wire. The outer saddle-shaped coil (75 mm O.D., 220 mm length) contained 12 turns (each) of 16/38 Litz Silk Served Wire.

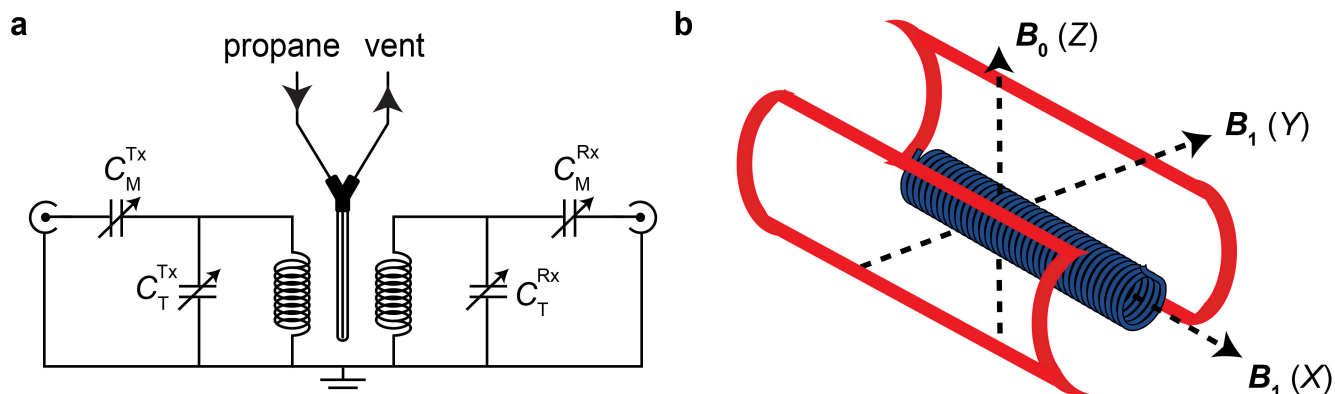


Figure S1. a) The RF probe circuit: two single channel circuits (Tx and Rx) with common ground tuned for ^1H . b) Alignment of RF coils, static and alternating magnetic fields.

The coils were shielded from electric field interference and noise by housing them in a hollow copper cube made out of square (1 ft \times 1 ft) copper clad PCB materials (Figure S2). A circular waveguide 50 mm in length was built to protrude from the shield to act as an access point for the sample to be inserted into the coil. The shielding provided an electric field suppression of 60 dB.

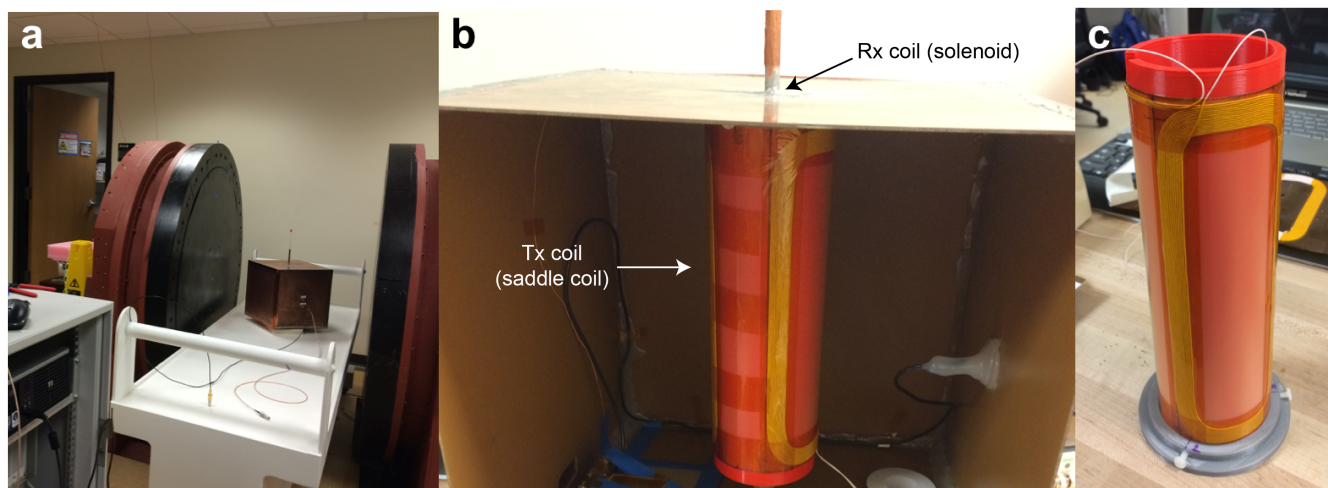


Figure S2. Photographs of (a) the permanent magnet (~ 0.05 T) with the dual-channel NMR probe centered in the homogeneous region of the magnet. (b) Dual-channel $^1\text{H}/^1\text{H}$ coil located inside the box (1 ft \times 1 ft \times 1 ft) made of copper clad PCB material. The shielding box was used for attenuation of an electric field providing suppression of 60 dB. (c) Outer saddle coil used for NMR signal excitation.

2. Spin dynamics calculations for the action of SLIC on propane

Simulations were carried out by numerically treating the Liouville–von Neumann equation for the spin density matrix. The initial density matrix of p -H₂ was constructed as $\hat{\rho}_{\text{H}_2} = \frac{1}{4} \hat{1} - \hat{\mathbf{I}}_1 \hat{\mathbf{I}}_2$. The density matrix of the propane molecule was constructed as a direct product between $\hat{\rho}_{\text{H}_2}$ and the unit matrix representing the thermally polarized 6-spin system of propylene (see Matlab code below). In order to account for averaging of coherences arising from the time dispersion of the polarization build-up process, only diagonal elements of the matrix written on the eigenbasis of the Hamiltonian were kept and all non-diagonal elements were discarded. The matrix obtained was converted back into the Zeeman basis, and exposed to the action of the Hamiltonian representing low-frequency continuous-wave (CW) RF field for a time τ_{SLIC} . Then the trace of the product of the operator \hat{I}_x and density matrix of the spin system was taken and plotted vs. B_1 amplitude (Hz) for a range of selected values of τ_{SLIC} . Note that relaxation effects were not included in the simulations.

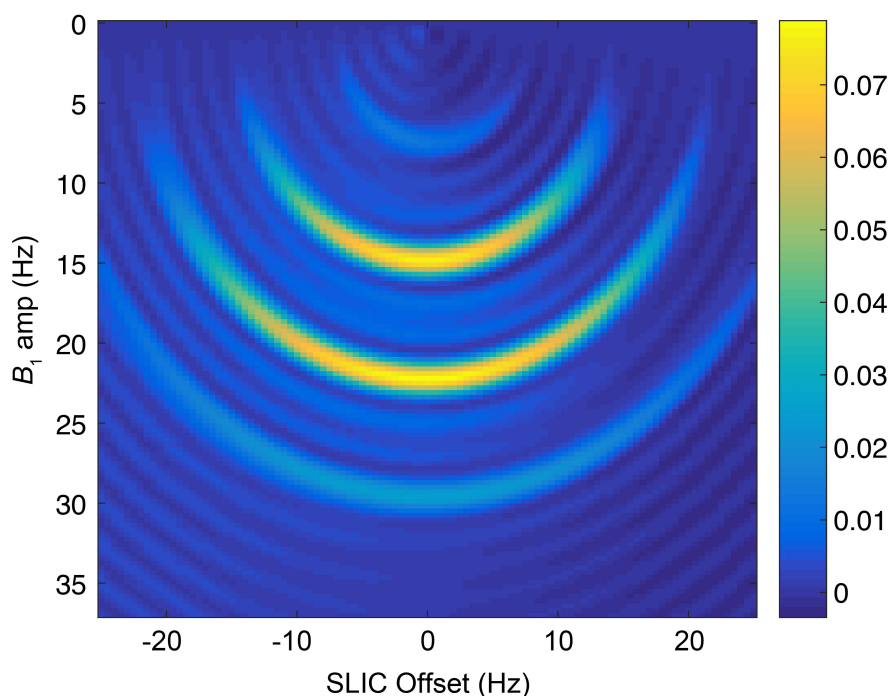


Figure S3. Simulation of ¹H NMR signal dependence for the 8-spin system of propane on SLIC parameters: B_1 amplitude (Hz) and pulse offset (Hz) (position of zero offset corresponds to the center between two resonances). SLIC pulse time is 0.5 s. NMR parameters of propane: $\delta_1 = 0.9$ ppm (CH₃ groups), $\delta_1 = 1.34$ ppm (CH₂ group), $J = 7.4$ Hz.

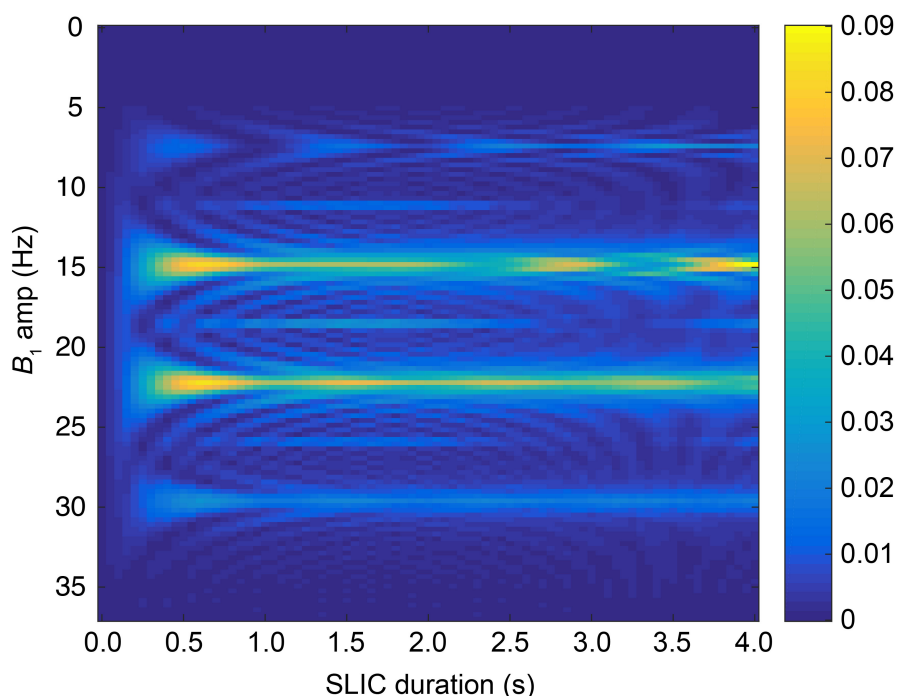


Figure S4. Simulation of ^1H NMR signal dependence for the 8-spin system of propane on B_1 amplitude (Hz) and SLIC pulse time (SLIC duration) at zero RF pulse offset (corresponding to the center frequency between CH_2 and CH_3 resonances). NMR parameters are the same as in Figure S3.

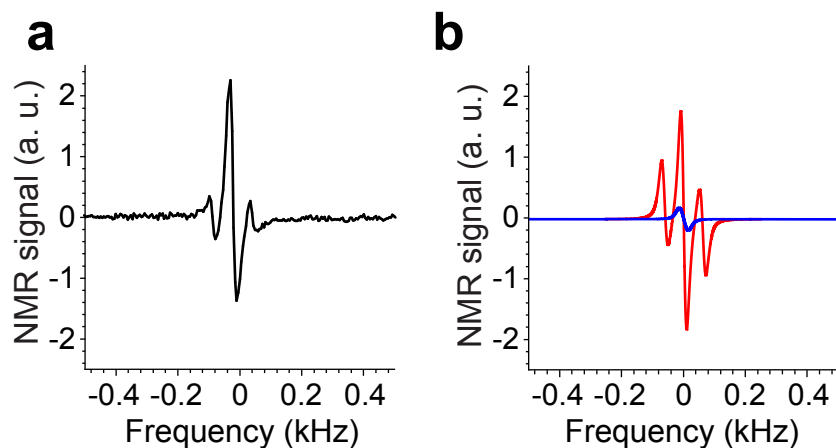


Figure S5. a) ^1H NMR spectrum of HP propane recorded at 0.05 T after application of a hard $\pi/4$ RF pulse; the spectrum is reprinted from Ref. [1]. b) Simulation of ^1H NMR spectrum of HP propane (after application of a hard $\pi/4$ RF pulse): blue trace – HP propane population without a ^{13}C nucleus, red trace – HP propane containing 1.1% (natural ^{13}C abundance) of randomly distributed ^{13}C nuclei.

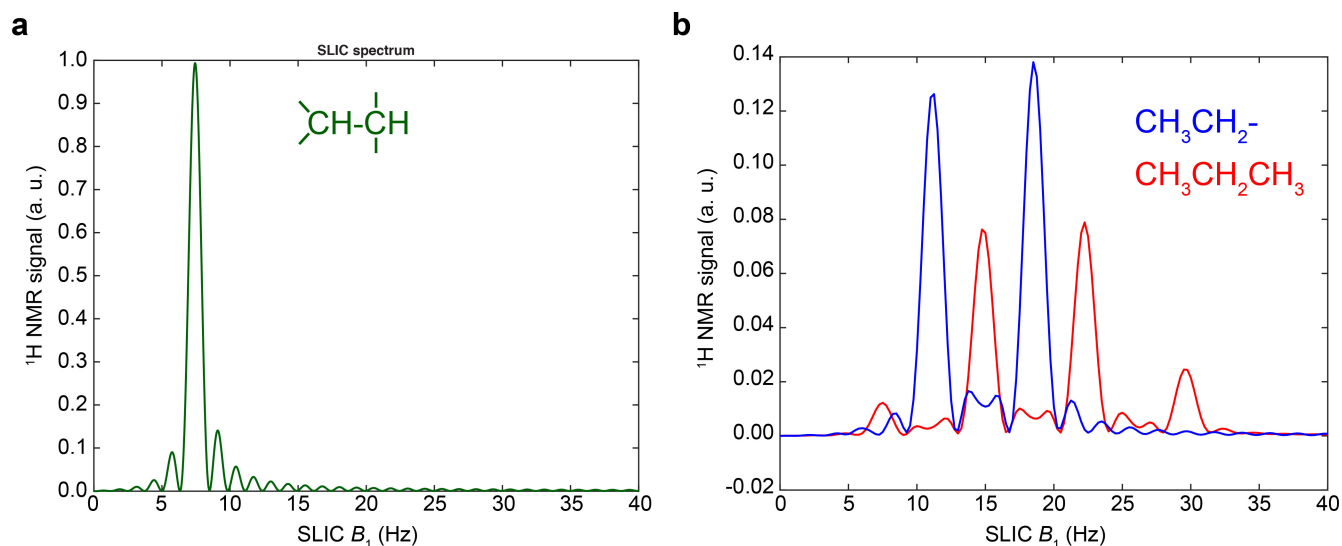


Figure S6. a) Theoretically calculated dependence of the SLIC-induced signal on B_1 amplitude for an isolated two proton-spin system in a hypothetical hydrocarbon motif using J coupling constant between two protons of 7.4 Hz, and the chemical shift difference ($\Delta\nu$) of 0.44 ppm. The SLIC RF pulse duration is 0.8035 s ($0.707/\Delta\nu$) and the magnetic field corresponds to 2.0 MHz. The maximum of ~ 1.0 is clearly seen at B_1 of 7.4 Hz. b) Theoretically calculated dependence of the SLIC-induced signal on B_1 amplitude for propane (red trace, same as in Figure 2e) and ethyl group (blue trace). J coupling constant between protons in CH_3- and CH_2- groups is 7.4 Hz in both calculations. The SLIC RF pulse duration is 0.5 s and the static magnetic field corresponds to 2.0 MHz. Note that y -values may not fully reflect the normalization coefficient which may be required. These values of SLIC conversion efficiency are provided for comparative purpose only.

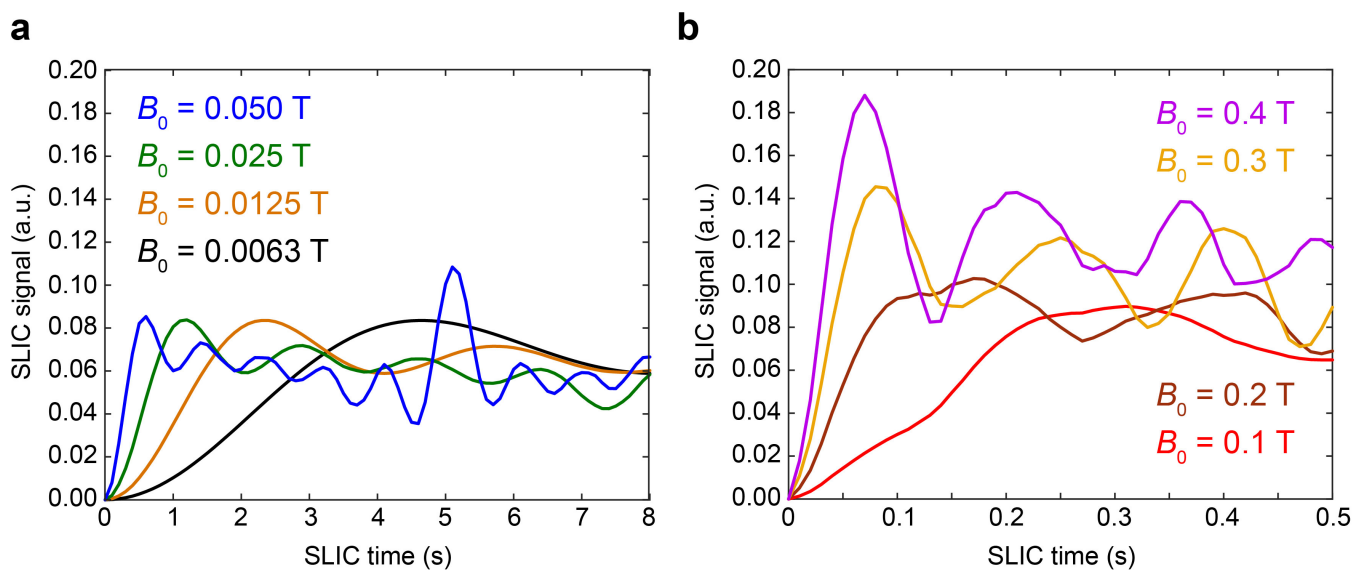


Figure S7. Simulation of ^1H NMR signal dependence for the 8-spin system of propane on SLIC pulse time (SLIC duration) at various static magnetic fields at zero RF pulse offset and B_1 of 22.2 Hz. NMR parameters are the same as in Figure S3. Note that relaxation effects were not included into simulation.

3. Analytical analysis of the ^1H NMR signal vs. SLIC duration at 0.05 T

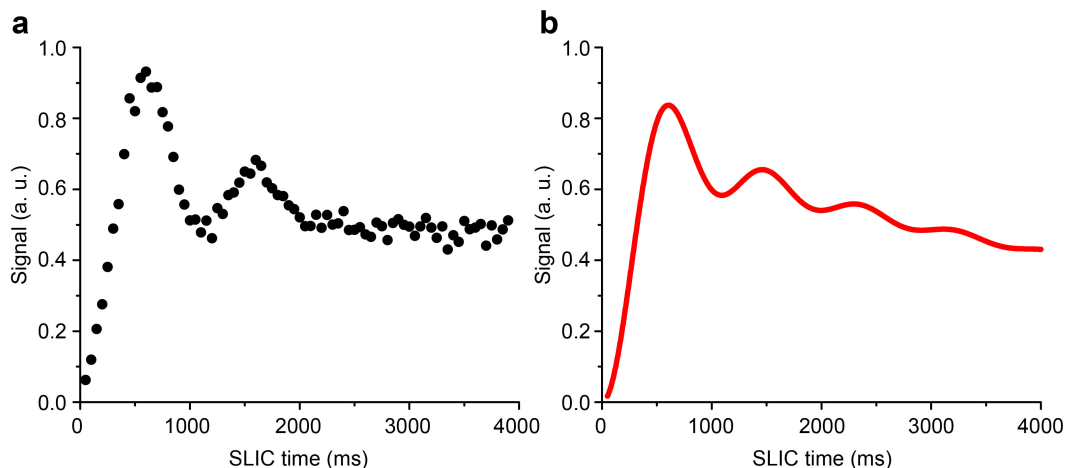


Figure S8. Dependence of ^1H NMR signal of HP propane on the SLIC duration: a) experimental data. b) fitting using the eq. (S2).

In the simple case of a two-spin system spin-lock induced singlet-triplet mixing leads to the following dependence of the magnetization (M_x) as a function of SLIC time (τ):²

$$M_x = \frac{1 - \cos(\omega\tau)}{2}$$

where ω is a frequency of singlet-triplet mixing determined by a chemical shift difference between p - H_2 -nascent protons. Our experimental geometry, where propane is constantly flowing through the detection zone of NMR spectrometer while being irradiated by a SLIC pulse, allows us to conveniently study its dependence of the irradiation duration using the parameter τ as a characteristic time spent in the detection chamber. In other words, we analyze the case where SLIC time is equal to the residence time $\tau = V/u$ of propane in the detection chamber (here V [mL] is the volume of the detection chamber, and u [mL/s] is the flow rate of propane). Since different HP propane molecules spend different amount of time in the detection zone, averaging over τ is necessary in order to obtain the resulting NMR signal as a function of SLIC time:

$$S = \frac{1}{\tau} \int_0^{\tau} \frac{1 - \cos(\omega t)}{2} dt = \frac{1}{2} \left(1 - \frac{\sin(\omega\tau)}{\omega\tau} \right) \quad (\text{eq. S1})$$

This equation does not take into account relaxation due to T_2 and other relaxation processes occurring during the action of a SLIC RF-pulse. In order to take this into account, eq. S1 should be modified as follows:

$$(\text{eq. S2})$$

$$S = \frac{1}{\tau} \int_0^{\tau} \frac{1 - \cos(\omega t)}{2} e^{-\frac{t}{T_2}} dt = \frac{1}{2\tau} \left\{ T_2 \left(1 - e^{-\frac{\tau}{T_2}} \right) - \frac{e^{-\frac{\tau}{T_2}} \left(\omega \cdot \sin(\omega\tau) - \left(\frac{1}{T_2} \right) \cos(\omega\tau) \right) + \frac{1}{T_2}}{\left(\omega^2 + \left(\frac{1}{T_2} \right)^2 \right)} \right\}$$

We note that this averaging is valid only for residence times shorter than SLIC time (*e.g.*, if residence time is much longer than τ , most spins would experience the full SLIC pulse). Figure S7 shows that experimentally found data points (Figure S7a) are in agreement with the fitting according to eq. S2 (Figure S7b). The following parameters were extracted from fitting: $\omega = 7.27 \pm 0.13$, $T_2 = 2.91 \pm 0.23$ s.

4. Values for T_1 and T_S and reaction conversion at different pressures

Table S1. Values of T_1 and T_S of propane measured at 0.05 T at various pressures.

Total pressure, atm	T_1 , s	T_S , s	T_S/T_1	Flow rates, sccm	
				C_3H_6	H_2
3.0	1.6±0.2	5.4±0.2	3.4±0.5	300	300
3.5	1.4±0.4	5.0±0.2	3.6±1.2	40	50
3.7	2.2±0.2	6.1±0.5	2.8±0.5	300	300
4.4	2.9±0.3	7.9±0.7	2.7±0.5	300	300
5.1	4.4±0.4	10.2±0.5	2.3±0.3	50	60
5.1	2.9±0.3	7.9±0.3	2.7±0.4	300	300
5.8	2.7±0.4	10.5±1.3	3.9±1.1	300	300
6.4	3.6±0.3	9.1±0.9	2.5±0.5	300	300
6.6	2.8±0.3	8.4±0.2	3.0±0.4	70	85
7.1	3.0±0.2	10.3±1.3	3.4±0.7	300	300
7.6	3.9±0.4	13.1±0.4	3.4±0.4	80	100
Average T_S/T_1 ratio			3.1±0.5		

Table S2. Reaction conversion calculated from gas composition measured at different reaction pressures using 1H NMR spectroscopy at 400 MHz.

Total pressure, atm	Conversion, %	Gas fractions		
		C_3H_6	H_2	C_3H_8
1.0	22.4	0.44	0.44	0.13
1.7	40.2	0.37	0.37	0.25
2.4	52.4	0.32	0.32	0.36
3.0	57.9	0.30	0.30	0.41
3.7	61.4	0.28	0.28	0.44
4.4	62.4	0.27	0.27	0.45
5.1	69.9	0.23	0.23	0.54
5.8	72.8	0.21	0.21	0.57
6.4	78.5	0.18	0.18	0.65
7.1	82.4	0.15	0.15	0.70

5. MatLab code used for the spin dynamics calculations

```
function [] = SLIC_dispersion_code()
% SLIC dispersion simulation program (propane)
% danila.barskiy@vanderbilt.edu

% Spin system parameters for propane
N_spins=8;
ppm=[0.9 0.9 0.9 1.34 1.34 0.9 0.9 0.9]; % chemical shifts of protons
J=7.4; % scalar coupling between CH3 and CH2 group (in Hz)
scalar_couplings=[0 0 0 J J 0 0 0; 0 0 0 J J 0 0 0; 0 0 0 J J 0 0 0; ...
                  0 0 0 0 0 J J J; 0 0 0 0 0 J J J; 0 0 0 0 0 0 0 0; ...
                  0 0 0 0 0 0 0 0; 0 0 0 0 0 0 0 0];

% Magnetic field and spectral parameters
v0=2*1e6; % Larmor frequency in Hz
ppm_ref=1.12; % center of the spectrum

% Changing indexes for 1st and 4th protons (they will be p-H2-nascent protons)
ppm([2 4])=ppm([4 2]);
scalar_couplings(:,[2 4])=scalar_couplings(:,[4 2]); % changing 2nd and 4th columns
scalar_couplings([2 4],:)=scalar_couplings([4 2],:); % changing 2nd and 4th rows
scalar_couplings=triu(scalar_couplings)+(scalar_couplings-triu(scalar_couplings))';
% let's put all elements above diagonal

% Offset frequencies (Hz) for all spins
v_freqs=v0*(ppm-ppm_ref)*1e-6;

% SLIC frequency offset (ppm) and amplitude (Hz)
v_RF = ppm_ref; % position of RF pulse
v_offset = v0*(v_RF-ppm_ref)*1e-6;
amp_rf=0:0.25:40;

% Define spin operators
[sigma_x, sigma_y, sigma_z, Lx, Ly, Lz]=Spin_Operator(N_spins);

% Initial state
rho_H2 = 0.25*eye(4)-
(kron(sigma_x,sigma_x)+kron(sigma_y,sigma_y)+kron(sigma_z,sigma_z)); % pH2-nascent
spins
E = (1/(2^(N_spins-2)))*eye(2^(N_spins-2)); % other spins in the molecule
rho=kron(rho_H2,E);

% Build Hamiltonian (before pulse is applied)
H = SLIC_Hamiltonian(Lx, Ly, Lz, v_freqs, v_offset, 0, scalar_couplings, N_spins);

% Simulation, stage 1: killing the coherences
[Eig_H, ~] = eig(H);
rho = Eig_H\rho*Eig_H; % density matrix in Hamiltonian eigenbasis
rho = rho.*eye(2^N_spins); % killing non-diagonal elements
rho = Eig_H*rho/Eig_H; % back to Zeeman basis

% Detection state
coil=zeros(2^N_spins,2^N_spins);
for n=1:N_spins
    coil=coil+Lx{n}+1i*Ly{n};
end
```

```

% Simulation, stage 2: SLIC pulse
tau_SLIC = 0.5; % in seconds
S = zeros(numel(amp_rf),1); % SLIC signal vs. B1
for k=1:numel(amp_rf)
H_SLIC = SLIC_Hamiltonian(Lx, Ly, Lz, v_freqs, v_offset, amp_rf(k),
scalar_couplings, N_spins);
P_SLIC=expm(-1i*2*pi*H_SLIC*tau_SLIC);
rho_after = P_SLIC*rho*P_SLIC';
S(k) = real(trace(coil*rho_after)); % SLIC signal
end

plot(amp_rf,S);
title('SLIC spectrum');
ylabel('SLIC signal (a.u.)');
xlabel('B1 amp (Hz)');

end

function H=SLIC_Hamiltonian(Lx, Ly, Lz, v_freqs, v_offset, B1_amp,
scalar_couplings, N_spins)
% Calculation of Hamiltonian matrix

% Preallocate Hamiltonian array
H=zeros(2^N_spins,2^N_spins);

% Zeeman interactions
for n=1:N_spins
H=H-(v_freqs(n)-v_offset)*Lz{n};
end

% Transverse interactions (B1 components)
for n=1:N_spins
H=H-B1_amp*Lx{n};
end

% Scalar couplings
for n=1:N_spins
for k=1:N_spins
H=H+(scalar_couplings(n,k))*(Lx{n}*Lx{k}+Ly{n}*Ly{k}+Lz{n}*Lz{k});
end
end

end

function [sigma_x, sigma_y, sigma_z, Lx, Ly, Lz]=Spin_Operator(N_spins)
% Calculation of set of spin operators on the basis of N_spins
% code is adapted from https://www.youtube.com/watch?v=ZgLqt44jW00

% Define Pauli matrices
sigma_x=[0 1/2; 1/2 0];
sigma_y=[0 -1i/2; 1i/2 0];
sigma_z=[1/2 0; 0 -1/2];
unit=[1 0; 0 1];

% Cell arrays operators
Lx=cell(1, N_spins); Ly=cell(1, N_spins); Lz=cell(1, N_spins);

% Define spin operators

```

```

for n=1:N_spins
  Lx_current=1; Ly_current=1; Lz_current=1;
  for k=1:N_spins
    if k==n
      Lx_current=kron(Lx_current,sigma_x);
      Ly_current=kron(Ly_current,sigma_y);
      Lz_current=kron(Lz_current,sigma_z);
    else
      Lx_current=kron(Lx_current, unit);
      Ly_current=kron(Ly_current, unit);
      Lz_current=kron(Lz_current, unit);
    end
  end
  Lx{n}=Lx_current; Ly{n}=Ly_current; Lz{n}=Lz_current;
end
end

```

6. References Used in Supporting Information

1. Kovtunov, K.; Truong, M.; Barskiy, D.; Koptyug, I.; Coffey, A.; Waddell, K.; Chekmenev, E. Long-Lived Spin States for Low-field Hyperpolarized Gas MRI. *Chem. Eur. J.* **2014**, *20*, 14629-32.
2. DeVience, S.; Walsworth, R.; Rosen, M. Preparation of Nuclear Spin Singlet States Using Spin-Lock Induced Crossing. *Phys. Rev. Lett.* **2013**, *111*, 173002.